HHS Public Access

Author manuscript

J Cell Biochem. Author manuscript; available in PMC 2016 October 01.

Published in final edited form as:

J Cell Biochem. 2015 October ; 116(10): 2354–2364. doi:10.1002/jcb.25186.

Protective role of Smad6 in inflammation-induced valvular cell calcification

Xin Li[1,#], **Jina J. Lim**[2,#], **Jinxiu Lu**[3], **Taylor M. Pedego**[1], **Linda Demer**[1,3,4], and **Yin Tintut**[1,*]

[1]Department of Medicine, University of California, Los Angeles, California

[2]Department of Pediatrics, University of California, Los Angeles, California

[3]Department of Physiology, University of California, Los Angeles, California

[4]Department of Bioengineering, University of California, Los Angeles, California

Abstract

Calcific aortic vascular and valvular disease (CAVD) is associated with hyperlipidemia, the effects of which occur through chronic inflammation. Evidence suggests that inhibitory small mothers against decapentaplegic (I-Smads; Smad6 and 7) regulate valve embryogenesis and may serve as a mitigating factor in CAVD. However, whether I-Smads regulate inflammation-induced calcific vasculopathy is not clear. Therefore, we investigated the role of I-Smads in atherosclerotic calcification. Results showed that expression of Smad6, but not Smad7, was reduced in aortic and valve tissues of hyperlipidemic compared with normolipemic mice, while expression of tumor necrosis factor alpha (TNF-a) was upregulated. To test whether the effects are in response to inflammatory cytokines, we isolated murine aortic valve leaflets and cultured valvular interstitial cells (mVIC) from the normolipemic mice. By immunochemistry, mVICs were strongly positive for vimentin, weakly positive for smooth muscle alpha actin, and negative for an endothelial cell marker. TNF-a upregulated alkaline phosphatase (ALP) activity and matrix mineralization in mVICs. By gene expression analysis, TNF-a significantly upregulated bone morphogenetic protein 2 (BMP-2) expression while downregulating Smad6 expression. Smad7 expression was not significantly affected. To further test the role of Smad6 on TNF-a-induced valvular cell calcification, we knocked down Smad6 expression using lentiviral transfection. In cells transfected with Smad6 shRNA, TNF-a further augmented ALP activity, expression of BMP-2, Wnt- and redox-regulated genes, and matrix mineralization compared with the control cells. These findings suggest that TNF-a induces valvular and vascular cell calcification, in part, by specifically reducing the expression of a BMP-2 signaling inhibitor, Smad6.

Keywords

Calcification; TNF-a; valvular cells; Smad6; BMP-2

[*]To whom correspondence should be addressed: Yin Tintut, Ph.D., The David Geffen School of Medicine, University of California, Los Angeles, Center for the Health Sciences A2-237, 10833 Le Conte Ave, Los Angeles, CA. 90095-1679, Phone: (310) 206-9964, Fax: (310) 825-4963, ytintut@mednet.ucla.edu.

[#]Co-first authors contributed equally to the work

INTRODUCTION

Calcific aortic vascular and valvular disease (CAVD) increases the risk of cardiovascular and all-cause mortality (Gondrie et al., 2011; O'Rourke et al., 2000; Rennenberg et al., 2009). It is widespread, with prevalence increasing with age; approximately 60% of 60 year-olds have coronary or aortic calcification (Budoff et al., 2007; Rennenberg et al., 2009). Calcification reduces compliance (Demer, 1991), leading to clinical consequences, such as hypertension, coronary ischemia, infarction, congestive heart failure, and ventricular hypertrophy (London et al., 2002; Shao et al., 2010). Its clinical severity is due to leaflet stiffening, which restricts valve opening, increasing outflow resistance and oxygen demand, while impairing cardiac perfusion and oxygen supply. Although CAVD is a rapidly fatal disorder, therapeutic options are extremely limited. Thus, a better understanding of the mechanisms underlying calcification and stiffening is critical for the development of early diagnosis and medical therapy.

CAVD is associated epidemiologically with hyperlipidemia, the biological effects of which appear to occur through an inflammatory, positive feedback loop linking oxidized lipids, cytokines, and oxidant stress. Higher levels of circulating inflammatory cytokines, such as tumor necrosis factor alpha (TNF-a), are associated with a higher prevalence of atherosclerosis (Bruunsgaard et al., 2000) and greater progression of aortic valve stenosis (Swierszcz et al., 2011). Serum TNF-a levels are also upregulated in the hyperlipidemic, low-density receptor deficient (Ldlr−/−) mice (Al-Aly et al., 2007; Pirih et al., 2012). Leukocyte infiltration and TNF-a transcripts have been located near calcium deposits in valve leaflets (Cote et al., 2013). In animal models, treatment of mice with anti-TNF-a antibody prevents high-fat diet-induced aortic calcification (Al-Aly et al., 2007). CAVD is increasingly acknowledged as a regulated process, involving osteochondrogenic differentiation of vascular and valvular cells. Inflammatory stimuli, such as cytokines and lipid oxidation products, promote the osteoblastic differentiation of vascular and valvular cells (Kaden et al., 2005; Lee et al., 2010; Parhami et al., 1997; Tintut et al., 2000; Yu et al., 2011).

BMP-2, a potent morphogen for myogenesis, adipogenesis, chondrogenesis, and osteogenesis, is crucial for early heart valve formation and regionalized myocardial patterning (Ma et al., 2005; Wang et al., 2013). We, and others, have shown that BMP-2 is found in human calcified atherosclerotic plaques (Bostrom et al., 1993; Dhore et al., 2001). It also co-localizes with the calcified surface of the valve leaflets, the valvular fibrosa (Mohler et al., 1999; Mohler et al., 2001). Overexpression of BMP-2 or stimulation of BMP-2 signaling cause increased valvular and vascular calcification (Nakagawa et al., 2010; Song et al., 2015), and inhibition of BMP-2 signaling causes reduced vascular calcification (Derwall et al., 2012), suggesting BMP-2 has a causal role in CAVD.

Evidence suggests that specific downstream targets of bone morphogenetic proteins (BMPs), known as inhibitory "small mothers against decapentaplegic" (I-Smads; Smad6 and 7), regulate valve embryogenesis and may serve as a mitigating factor in CAVD. Two of their upstream effectors, bone morphogenetic protein-2 (BMP-2) and transforming growth factor-beta (TGF-b), are expressed in CAVD (Bostrom et al., 1993; Watson et al., 1994). Findings

in Smad6 null mice that develop aortic valvular cartilage and calcium mineral deposits suggest that Smad6 protects against vascular and valvular calcification (Galvin et al., 2000). It is not clear whether these effects are due to changes in smooth muscle cells, valvular interstitial cells, endothelial cells, and/or cells in the adventitial layer. Therefore, in this study, we investigated the mechanism of the protective role of Smad6 by valvular cells in response to inflammatory insults, such as TNF-a.

MATERIALS AND METHODS

Materials

Human TNF-a was from R&D Systems. Antibodies to tubulin and vimentin were from Cell Signaling (MA), to smooth muscle alpha actin and Smad7 were from Santa Cruz Biotechnology (CA), to Smad6 were from Imgenex, to anti-TNF-a were from Abcam, and to anti-von Willebrand factor (vWF) was from Dako (CA). Lentiviral constructs for control (scrambled) and Smad6 shRNA were from Santa Cruz Biotechnology (CA).

Tissue isolation

All the experimental protocols were reviewed and approved by the Institutional Animal Care and Use Committee of the University of California at Los Angeles. Aortic tissues from 6 to 8-month-old male C57BL/6 (n = 5) and $Ldlr^{-/-}$ (n = 5) mice were dissected, cleaned of surrounding tissues, homogenized, and total RNA was isolated using TRIzol reagent (Invitrogen). $Ldlr^{-/-}$ mice were on a C57BL/6 background, and all the mice were on a standard chow diet. Mouse sera were collected at necropsy. The serum levels of total and HDL cholesterol were performed by UCLA Division of Laboratory Animal Medicine using ACE Alera Clinical Chemistry System, and the levels of LDL cholesterol were a calculated value.

Cell culture

Valve leaflets were excised from C57BL/6 mice, and valvular interstitial cells were cultured on collagen/gelatin-coated plates via an explant technique. Aortic smooth muscle cells were isolated, as previously described (Huang et al., 2008). Both cell types were maintained in Dulbecco's Modified Eagle's Medium (DMEM; Cellgro) supplemented with 20% FBS. For osteoblastic differentiation, cells (passages 8–11) were cultured in alpha-MEM media (aMEM; Cellgro) supplemented with 10% FBS, penicillin, streptomycin, sodium pyruvate, 5 mM beta-glycerophosphate and 50 μg/ml ascorbic acid with the indicated agent. Media were replaced with fresh agents every 3 – 4 days. Where indicated, cells were treated with pyrrolidine dithiocarbamate (PDTC: 10 μM) or pre-treated with Trolox (400 μM) for 1 hr prior to TNF-a addition at each media change.

Lentiviral transfection

Lentiviral transfection was performed, following the manufacturer's instructions. Briefly, cells were transfected at approximately 50% confluency with lentiviral particles carrying either control shRNA, Smad6 shRNA, or BMP-2 shRNA overnight, and the stable clones expressing the shRNA were selected in media containing puromycin dihydrochloride (2 μg/ml puromycin).

Immunofluorescence

For Smad6 and TNF-a expression in aortic tissues, aortic roots from 10–11 month-old C57BL/6 (n = 8) and $Ldlr^{-/-}$ (n = 6) mice were fixed and stained with anti-Smad6 or anti-TNF-a antibodies and visualized using secondary antibody conjugated with Alex Fluor 555. Fluorescence intensity of the images were quantified and normalized per tissue area in 2 sections per aortic root using image analysis software (Metamorph Advanced *v*7.7). For identification of mVICs, cells were plated in 8-well chamber slides and at confluence, the cells were washed, fixed, incubated overnight with anti-vimentin, anti-vWF, or smooth muscle alpha-actin antibodies, and visualized using secondary antibody conjugated with Alexa Fluor 488.

Alkaline phosphatase activity

Alkaline phosphatase activity was assessed via cytochemical staining, quantified by Metamorph image analysis, and normalized to total number of cells (DAPI nuclear stain). The assay was performed in quintuplicate wells.

Matrix calcification

Cells were incubated overnight in 0.6 N hydrogen chloride and matrix calcium levels (normalized to total protein) were analyzed by the *o*-cresolphthalein complexone method (Teco Diagnostics) in quintuplicate (Huang et al., 2008).

RNA isolation and realtime RT-qPCR

Total RNA was isolated using TRIzol reagent. Real-time PCR was performed using gene specific primers, One-Step qRT-PCR SuperMix Kit (BioChain Inc.) and Mx3005P (Stratagene). Values were normalized to beta-actin. Primer sequences were ALP, forward primer: 5′-CCAACTCTTTTGTGCCAGAGA-3′, reverse primer: 5′ GGCTACATT GGTGTTGAGCTTTT-3′; BMP-2, forward primer: 5′-TGTCCAATCCGTGAGAAC-3′, reverse primer: 5′-TGCCATCATCACTTCCTG-3′; TNF-a, forward primer: 5′-GCCAGTGAGTGAAAGGGACAG-3′, reverse primer: 5′-GCCAGGAGGGAGAACAGAAAC-3′; Smad6, forward primer: 5′-CCACTGGAT CTGTCCGATTCT-3′, reverse primer: 5′-GGTCGTACACCGCATAGAGG-3′; and Smad7, forward primer: 5′-ATCTTCATCAAGTCCGCCAC-3′, reverse primer: 5′-AACCAGGGAACACTTTGTGC-3′; catalase, forward primer: 5′-AGCGACCAGATGAAGCAGTG-3′, reverse primer: 5′-TCCGCTCTC TGTCAAAGTGTG-3′; heme oxygenase 1, forward primer: 5′-AAGCCGAGAATGCTGAGTTCA-3′, reverse primer: 5′-GCCGTGTAGATATGGTACAAGGA-3′; Axin-2, forward primer: 5′-TGACTCTCCTTCCAGATCCCA-3′, reverse primer: 5′-TGCCCACACTAGGCTGACA-3′; lymphoid enhancer-binding factor-1 (LEF-1), forward primer: 5′-TGTTTATCCCATCACGGGTGG-3′, reverse primer: 5′-CATGGAAGTGTCGCCTGACAG-3′.

Western analysis

Western analysis of whole cell lysates was performed using standard protocols. Quantification was performed using NIH Image J *v64*.

Statistical analysis

Experiments (≥ quadruplicate wells) were performed ≥ 3 times, and data are expressed as mean ± SEM. Results were compared using a two-tailed, Student's *t*-test. In comparisons across more than two groups, two-way ANOVA, followed by Fisher's PLSD, was performed. $p < 0.05$ was considered statistically significant.

RESULTS

Effects of hyperlipidemia on I-Smads and TNF-a expression

To assess the effects of hyperlipidemia on I-Smad and TNF-a expression, we isolated heart and aortic tissues from normolipemic (C57BL/6) and genetically hyperlipidemic ($Ldlr^{-/-}$) mice. As shown in Figure 1a, serum levels of total and LDL-cholesterol, but not HDL-cholesterol, were approximately 3- and 8-fold, respectively, higher in $Ldlr^{-/-}$ mice than in C57BL/6 mice. Realtime RT-qPCR analysis of RNA from aortic tissues of C57BL/6 and $Ldlr^{-/-}$ mice showed that expression of Smad6 was reduced by approximately 75% while aortic TNF-a expression was induced 190% in hyperlipidemic $Ldlr^{-/-}$ mice compared with normolipemic C57BL/6 mice (Fig. 1b). Expression of Smad7 was not altered by hyperlipidemia (Fig. 1b). Since mouse valve leaflets do not provide enough material for standard Western analysis, we performed immunofluorescence analysis of aortic roots from C57BL/6 and $Ldlr^{-/-}$ mice. As shown in Figure 1c–d, Smad6 and 7 were detected in both aortic valve leaflets and ascending aorta. Levels of Smad6, but not Smad7, were reduced in $Ldlr^{-/-}$ compared with C57BL/6 mice. In contrast, TNF-a protein levels were upregulated in aortic valve leaflets of $Ldlr^{-/-}$ mice (Fig. 1e).

Effects of TNF-a on osteoblastic differentiation and mineralization

To test the direct effects of TNF-a on Smad6 expression, we isolated murine aortic valve leaflets from C57BL/6 mice and cultured valvular interstitial cells (mVIC). Imunofluorescence analyses of mVICs revealed that the cells are strongly positive for vimentin, weakly positive for smooth muscle alpha actin, and negative for vWF, an endothelial cell marker (data not shown). These results are consistent with the findings in porcine valvular interstitial cells (Chen et al., 2009).

Treatment of the mVICs isolated from male mice with TNF-a upregulated alkaline phosphatase (ALP) activity and matrix mineralization (Fig. 2a). Gene expression analysis showed that TNF-a significantly upregulated expression of ALP and BMP-2, while it down-regulated Smad6 expression by 30% (Fig. 2b). Smad7 expression was not significantly affected by TNF-a (Fig. 2b). Western blot analysis showed TNF-a inhibited Smad6 expression by approximately 40% (Fig. 2c). In murine aortic smooth muscle cells, TNF-a also inhibited Smad6 expression by approximately 25%, whereas Smad7 expression was not significantly altered (data not shown).

To test whether the effects are gender dependent, we isolated mVIC from female mice, and the experiments were repeated. Results showed similar trends in the cells from female mice (data not shown), suggesting that the effects are gender independent.

To test whether the TNF-a inhibition of Smad6 is mediated through BMP-2, the cells were treated directly with BMP-2 and their expression of Smad6 and Smad7 was assessed. Results showed that, in contrast to the effects of TNF-a on expression of these I-Smads, BMP-2 treatment upregulated both Smad6 and Smad7 expression (Fig. 3a). To further test BMP-2 independent effects of Smad6 downregulation by TNF-a, we knocked down BMP-2 in these cells using lentiviral transfection of either control scrambled shRNA or BMP-2 shRNA. Realtime RT-qPCR analysis confirmed that BMP-2 mRNA expression levels were lowered by 50%. In these cells, TNF-a continued to inhibit Smad6 expression in BMP-2 knockdown cells (Fig. 3b), suggesting that inhibitory effects of TNF-a on Smad6 expression are indeed independent of BMP-2.

Effects of Smad6 knockdown on TNF-a-induced osteoblastic differentiation and mineralization

To further test the role of Smad6 on TNF-a-induced valvular cell calcification, we knocked down Smad6 expression using lentiviral transfection of either control or Smad6 shRNA. Realtime RT-qPCR and Western analyses show that Smad6 levels were reduced by approximately 50% (Fig. 4a–b).

In cells that had been transfected with Smad6 shRNA, TNF-a further augmented ALP activity and matrix mineralization beyond those seen in the control cells (Fig. 5a–b). In the absence of exogenous hTNF-a, long-term cultures (22 d) of Smad6 knockdown cells also had significantly more matrix mineralization (36%; $p < 0.05$) than control cells. Interestingly, gene expression analysis showed that basal ALP expression was higher in Smad6 knockdown cells (Fig. 5c). However, the fold-induction of ALP expression level by TNF-a was similar in both control and Smad6 knockdown cells (Fig. 5c). In contrast, gene expression analysis also showed that basal BMP-2 expression levels were similar in cells with control shRNA vs. Smad6 shRNA (Fig. 5c). However, the fold-induction of BMP2 expression level by TNF-a was augmented in Smad6 shRNA cells compared with control shRNA cells (Fig. 5c). Altogether, these findings, for ALP and BMP2, suggest that regulation is at the level of basal expression for ALP and at the level of TNF-a for BMP-2. Smad7 expression was not reduced by TNF-a in Smad6 shRNA knock down cells (Fig. 5c).

Since reactive oxygen species (ROS) and Wnt signaling are key downstream mediators of TNF-a effects (Lai et al., 2012), we tested whether oxidative stress mediates TNF-a inhibitory effects on Smad6 and/or Smad6 knockdown augments oxidative stress in mVICs. Results from realtime RT-qPCR showed that TNF-a-mediated reduction of Smad6 was not reversed by treating the mVICs with either of the antioxidants, Trolox or pyrrolidine dithiocarbamate (Fig. 6a). In contrast, TNF-a-induced redox-regulated genes (catalase and hemeoxygenase 1 (HO-1)) were further enhanced in Smad6 knockdown cells compared with the control cells (Fig. 6b). Similarly, Wnt-regulated genes (Axin-2 and LEF-1) were further augmented in Smad6 knockdown cells compared with the control cells (Fig. 6c).

DISCUSSION

In chronic inflammatory conditions such as atherosclerosis, cytokines such as TNF-a have been shown to induce ectopic calcification in the vasculature (Kaden et al., 2005; Lee et al., 2010; Tintut et al., 2000; Yu et al., 2011). We, and others, have found that both vascular cells, mainly comprised of smooth muscle cells, and valvular cells, mainly comprised of valvular interstitial cells, follow osteogenic differentiation and mineralization patterns that are similar to those of skeletal-derived bone cells (Mohler et al., 1999; Mohler et al., 2001; Tintut et al., 1998). The procalcific action of TNF-a on vascular and valvular cells appears to involve several mechanisms. TNF-a induces mineralization through an *indirect,* paracrine mechanism: induction of BMP-2 expression in endothelial cells (Buendia et al., 2014). TNF-a also induces mineralization through *direct,* autocrine mechanisms: augmentation of BMP-2 expression, as shown in the present study and by other investigators (Yu et al., 2011) and activation of the Msx2/Wnt signaling pathway (Al-Aly et al., 2007) in valvular and vascular mesenchymal cells. The present findings now suggest a third mechanism of action of TNF-a on vascular and valvular calcification: reduction of the BMP-2 inhibitor, Smad6.

Interestingly, the in vivo reduction in Smad6 caused by hyperlipidemia was greater than the in vitro reduction in Smad6 caused by TNF-a treatment. This may be attributable to hyperlipidemia inducing a variety of inflammatory cytokines, in addition to TNF-a. The effects of multiple cytokines may be additive or even synergistic. Smad6 regulation may also occur at additional levels beyond transcription, such as phosphorylation or cellular translocation of Smad6 after TNF-a exposure. It has been shown that in cancer cells, Smad6 is one of the targets of protein kinase X, and that phospho-Smad6 translocates to the nuclear compartment during macrophage differentiation (Glesne and Huberman, 2006).

We, and others, have previously found that *serum levels* of TNF-a were higher in hyperlipidemic than in normolipemic mice (Al-Aly et al., 2007; Pirih et al., 2012). In this study, we also found that *tissue levels* of TNF-a mRNA were higher in the aortas of hyperlipidemic mice. This is in agreement with the study by Cote and colleagues, who showed that TNF-a transcripts were present in calcified aortic valve tissue and that the density of inflammatory cells correlated with progression of stenosis (Cote et al., 2013). This evidence supports the concept that inflammatory factors act both systemically and locally.

Fukui and colleagues have previously shown that, in chondrocytes, TNF-a regulates BMP-2 transcripts by stabilizing mRNA post-transcriptionally via multiple pentameric AUUUA motifs in the 3′ untranslated regions (Fukui et al., 2006). Our findings in Smad6 knockdown cells support such a regulatory mechanism. Although BMP-2 autoregulates its own expression (Harris et al., 1994), in the absence of TNF-a, BMP-2 expression was not augmented in Smad6 knockdown cells, and TNF-a induced BMP-2 expression 3.6-fold in Smad6 knockdown cells compared with control knockdown cells (2.7-fold). This is in contrast to ALP expression, where the basal level of ALP was higher in the Smad6 knockdown cells compared with the control cells. One possibility is that BMP-2, present in the fetal bovine serum added to the culture medium, induced basal ALP expression. Also,

this may explain why calcification in Smad6 knockdown cells requires longer-term cultures in the absence of TNF-a.

Based on the important previous findings from Towler and colleagues, that TNF-a upregulates redox (Lai et al., 2012) and Wnt (Cheng et al., 2014) regulatory programs in aortic myofibroblast cells, together with evidence that BMP-2 acts through ROS to induce osteoblastic differentiation in bone-derived osteoblasts (Mandal et al., 2011), we considered the role of Smad6 in this signaling. The present results indicate that ROS production in response to TNF-a treatment is not required for Smad6 suppression and that Smad6 knockdown induces redox- and Wnt target genes. Altogether, these findings suggest that BMP-2 signaling through Smad6 is a proximal mediator of redox and Wnt regulatory programs.

The present findings also suggest that local production of TNF-a, which mitigates the intracellular Smad6 defense, appears to contribute more to osteogenic action than BMP-2 endocrine “tone.” This is, in part, because BMP-2 signaling upregulates its own inhibitor, Smad6, as part of negative feedback regulation. Our findings in Smad6 knockdown cells suggest that reduced Smad6 levels cause greater osteogenic activity than control knockdown cells, as well as a greater increase in osteogenic activity in response to TNF-a than control knockdown cells, all despite equal levels of BMP-2 endocrine tone from the fetal bovine serum.

In summary, these findings suggest a novel mechanism of action of TNF-a on vascular and valvular calcification: reduction of the BMP-2 inhibitor, Smad6. This mechanism may account for the cartilaginous metaplasia and ossification observed in aortic tissues of Smad6-null mice. Our findings also suggest that the ectopic vascular and valvular calcification may be exacerbated in the context of inflammation.

Acknowledgments

This work was supported by funding from the National Institutes of Health (DK081346, DK081346-S1, HL114709, and the National Center for Advancing Translational Sciences UCLA CTSI Grant UL1TR000124). T.M.P. was supported by the Jerome S. Tobis Fund for Medical Research.

Contract grant number: The National Institutes of Health (DK081346, DK081346-S1, HL114709, and the National Center for Advancing Translational Sciences UCLA CTSI Grant UL1TR000124).

References

Al-Aly Z, Shao JS, Lai CF, Huang E, Cai J, Behrmann A, Cheng SL, Towler DA. Aortic Msx2-Wnt calcification cascade is regulated by TNF-alpha-dependent signals in diabetic Ldlr−/− mice. Arterioscler Thromb Vasc Biol. 2007; 27:2589–2596. [PubMed: 17932314]

Bostrom K, Watson KE, Horn S, Wortham C, Herman IM, Demer LL. Bone morphogenetic protein expression in human atherosclerotic lesions. J Clin Invest. 1993; 91:1800–1809. [PubMed: 8473518]

Bruunsgaard H, Skinhoj P, Pedersen AN, Schroll M, Pedersen BK. Ageing, tumour necrosis factor-alpha (TNF-alpha) and atherosclerosis. Clinical and experimental immunology. 2000; 121:255–260. [PubMed: 10931139]

Budoff MJ, Shaw LJ, Liu ST, Weinstein SR, Mosler TP, Tseng PH, Flores FR, Callister TQ, Raggi P, Berman DS. Long-term prognosis associated with coronary calcification: observations from a registry of 25,253 patients. J Am Coll Cardiol. 2007; 49:1860–1870. [PubMed: 17481445]

Buendia P, Montes de Oca A, Madueno JA, Merino A, Martin-Malo A, Aljama P, Ramirez R, Rodriguez M, Carracedo J. Endothelial microparticles mediate inflammation-induced vascular calcification. FASEB J. 2014; 29:173–81. [PubMed: 25342130]

Chen JH, Yip CY, Sone ED, Simmons CA. Identification and characterization of aortic valve mesenchymal progenitor cells with robust osteogenic calcification potential. Am J Pathol. 2009; 174:1109–1119. [PubMed: 19218344]

Cheng SL, Behrmann A, Shao JS, Ramachandran B, Krchma K, Bello Arredondo Y, Kovacs A, Mead M, Maxson R, Towler DA. Targeted reduction of vascular Msx1 and Msx2 mitigates arteriosclerotic calcification and aortic stiffness in LDLR-deficient mice fed diabetogenic diets. Diabetes. 2014; 63:4326–4337. [PubMed: 25056439]

Cote N, Mahmut A, Bosse Y, Couture C, Page S, Trahan S, Boulanger MC, Fournier D, Pibarot P, Mathieu P. Inflammation is associated with the remodeling of calcific aortic valve disease. Inflammation. 2013; 36:573–581. [PubMed: 23225202]

Demer LL. Effect of calcification on in vivo mechanical response of rabbit arteries to balloon dilation. Circulation. 1991; 83:2083–2093. [PubMed: 2040058]

Derwall M, Malhotra R, Lai CS, Beppu Y, Aikawa E, Seehra JS, Zapol WM, Bloch KD, Yu PB. Inhibition of bone morphogenetic protein signaling reduces vascular calcification and atherosclerosis. Arterioscler Thromb Vasc Biol. 2012; 32:613–622. [PubMed: 22223731]

Dhore CR, Cleutjens JP, Lutgens E, Cleutjens KB, Geusens PP, Kitslaar PJ, Tordoir JH, Spronk HM, Vermeer C, Daemen MJ. Differential expression of bone matrix regulatory proteins in human atherosclerotic plaques. Arterioscler Thromb Vasc Biol. 2001; 21:1998–2003. [PubMed: 11742876]

Fukui N, Ikeda Y, Ohnuki T, Hikita A, Tanaka S, Yamane S, Suzuki R, Sandell LJ, Ochi T. Pro-inflammatory cytokine tumor necrosis factor-alpha induces bone morphogenetic protein-2 in chondrocytes via mRNA stabilization and transcriptional up-regulation. J Biol Chem. 2006; 281:27229–27241. [PubMed: 16835229]

Galvin KM, Donovan MJ, Lynch CA, Meyer RI, Paul RJ, Lorenz JN, Fairchild-Huntress V, Dixon KL, Dunmore JH, Gimbrone MA Jr, Falb D, Huszar D. A role for smad6 in development and homeostasis of the cardiovascular system. Nat Genet. 2000; 24:171–174. [PubMed: 10655064]

Glesne D, Huberman E. Smad6 is a protein kinase X phosphorylation substrate and is required for HL-60 cell differentiation. Oncogene. 2006; 25:4086–4098. [PubMed: 16491121]

Gondrie MJ, van der Graaf Y, Jacobs PC, Oen AL, Mali WP. The association of incidentally detected heart valve calcification with future cardiovascular events. Eur Radiol. 2011; 21:963–973. [PubMed: 21058039]

Harris SE, Bonewald LF, Harris MA, Sabatini M, Dallas S, Feng JQ, Ghosh-Choudhury N, Wozney J, Mundy GR. Effects of transforming growth factor beta on bone nodule formation and expression of bone morphogenetic protein 2, osteocalcin, osteopontin, alkaline phosphatase, and type I collagen mRNA in long-term cultures of fetal rat calvarial osteoblasts. J Bone Miner Res. 1994; 9:855–863. [PubMed: 8079661]

Huang MS, Sage AP, Lu J, Demer LL, Tintut Y. Phosphate and pyrophosphate mediate PKA-induced vascular cell calcification. Biochem Biophys Res Commun. 2008; 374:553–558. [PubMed: 18655772]

Kaden JJ, Kilic R, Sarikoc A, Hagl S, Lang S, Hoffmann U, Brueckmann M, Borggrefe M. Tumor necrosis factor alpha promotes an osteoblast-like phenotype in human aortic valve myofibroblasts: a potential regulatory mechanism of valvular calcification. Int J Mol Med. 2005; 16:869–872. [PubMed: 16211257]

Lai CF, Shao JS, Behrmann A, Krchma K, Cheng SL, Towler DA. TNFR1-Activated Reactive Oxidative Species Signals Up-Regulate Osteogenic Msx2 Programs in Aortic Myofibroblasts. Endocrinology. 2012; 153:3897–3910. [PubMed: 22685265]

Lee HL, Woo KM, Ryoo HM, Baek JH. Tumor necrosis factor-alpha increases alkaline phosphatase expression in vascular smooth muscle cells via MSX2 induction. Biochem Biophys Res Commun. 2010; 391:1087–1092. [PubMed: 20004646]

London GM, Marchais SJ, Guerin AP, Metivier F. Impairment of arterial function in chronic renal disease: prognostic impact and therapeutic approach. Nephrol Dial Transplant. 2002; 17(Suppl 11):13–15. [PubMed: 12386250]

Ma L, Lu MF, Schwartz RJ, Martin JF. Bmp2 is essential for cardiac cushion epithelial-mesenchymal transition and myocardial patterning. Development. 2005; 132:5601–5611. [PubMed: 16314491]

Mandal CC, Ganapathy S, Gorin Y, Mahadev K, Block K, Abboud HE, Harris SE, Ghosh-Choudhury G, Ghosh-Choudhury N. Reactive oxygen species derived from Nox4 mediate BMP2 gene transcription and osteoblast differentiation. Biochem J. 2011; 433:393–402. [PubMed: 21029048]

Mohler ER 3rd, Chawla MK, Chang AW, Vyavahare N, Levy RJ, Graham L, Gannon FH. Identification and characterization of calcifying valve cells from human and canine aortic valves. J Heart Valve Dis. 1999; 8:254–260. [PubMed: 10399657]

Mohler ER 3rd, Gannon F, Reynolds C, Zimmerman R, Keane MG, Kaplan FS. Bone formation and inflammation in cardiac valves. Circulation. 2001; 103:1522–1528. [PubMed: 11257079]

Nakagawa Y, Ikeda K, Akakabe Y, Koide M, Uraoka M, Yutaka KT, Kurimoto-Nakano R, Takahashi T, Matoba S, Yamada H, Okigaki M, Matsubara H. Paracrine osteogenic signals via bone morphogenetic protein-2 accelerate the atherosclerotic intimal calcification in vivo. Arterioscler Thromb Vasc Biol. 2010; 30:1908–1915. [PubMed: 20651281]

O'Rourke RA, Brundage BH, Froelicher VF, Greenland P, Grundy SM, Hachamovitch R, Pohost GM, Shaw LJ, Weintraub WS, Winters WL Jr, Forrester JS, Douglas PS, Faxon DP, Fisher JD, Gregoratos G, Hochman JS, Hutter AM Jr, Kaul S, Wolk MJ. American College of Cardiology/American Heart Association Expert Consensus document on electron-beam computed tomography for the diagnosis and prognosis of coronary artery disease. Circulation. 2000; 102:126–140. [PubMed: 10880426]

Parhami F, Morrow AD, Balucan J, Leitinger N, Watson AD, Tintut Y, Berliner JA, Demer LL. Lipid oxidation products have opposite effects on calcifying vascular cell and bone cell differentiation. A possible explanation for the paradox of arterial calcification in osteoporotic patients. Arterioscler Thromb Vasc Biol. 1997; 17:680–687. [PubMed: 9108780]

Pirih F, Lu J, Ye F, Bezouglaia O, Atti E, Ascenzi MG, Tetradis S, Demer L, Aghaloo T, Tintut Y. Adverse effects of hyperlipidemia on bone regeneration and strength. J Bone Miner Res. 2012; 27:309–318. [PubMed: 21987408]

Rennenberg RJ, Kessels AG, Schurgers LJ, van Engelshoven JM, de Leeuw PW, Kroon AA. Vascular calcifications as a marker of increased cardiovascular risk: a meta-analysis. Vasc Health Risk Manag. 2009; 5:185–197. [PubMed: 19436645]

Shao JS, Cheng SL, Sadhu J, Towler DA. Inflammation and the osteogenic regulation of vascular calcification: a review and perspective. Hypertension. 2010; 55:579–592. [PubMed: 20101002]

Song R, Fullerton DA, Ao L, Zheng D, Zhao KS, Meng X. BMP-2 and TGF-beta1 mediate biglycan-induced pro-osteogenic reprogramming in aortic valve interstitial cells. J Mol Med (Berl). 2015; 93:403–412. [PubMed: 25412776]

Swierszcz J, Dubiel JS, Krzysiek J, Sztefko K. One-year observation of inflammatory markers in patients with aortic valve stenosis. J Heart Valve Dis. 2011; 20:639–649. [PubMed: 22655494]

Tintut Y, Parhami F, Bostrom K, Jackson SM, Demer LL. cAMP stimulates osteoblast-like differentiation of calcifying vascular cells. Potential signaling pathway for vascular calcification. J Biol Chem. 1998; 273:7547–7553. [PubMed: 9516456]

Tintut Y, Patel J, Parhami F, Demer LL. Tumor necrosis factor-alpha promotes in vitro calcification of vascular cells via the cAMP pathway. Circulation. 2000; 102:2636–2642. [PubMed: 11085968]

Wang Y, Wu B, Chamberlain AA, Lui W, Koirala P, Susztak K, Klein D, Taylor V, Zhou B. Endocardial to myocardial notch-wnt-bmp axis regulates early heart valve development. PLoS One. 2013; 8:e60244. [PubMed: 23560082]

Watson KE, Bostrom K, Ravindranath R, Lam T, Norton B, Demer LL. TGF-beta 1 and 25-hydroxycholesterol stimulate osteoblast-like vascular cells to calcify. J Clin Invest. 1994; 93:2106–2113. [PubMed: 8182141]

Yu Z, Seya K, Daitoku K, Motomura S, Fukuda I, Furukawa K. Tumor necrosis factor-alpha accelerates the calcification of human aortic valve interstitial cells obtained from patients with

calcific aortic valve stenosis via the BMP2-Dlx5 pathway. J Pharmacol Exp Ther. 2011; 337:16–23. [PubMed: 21205918]

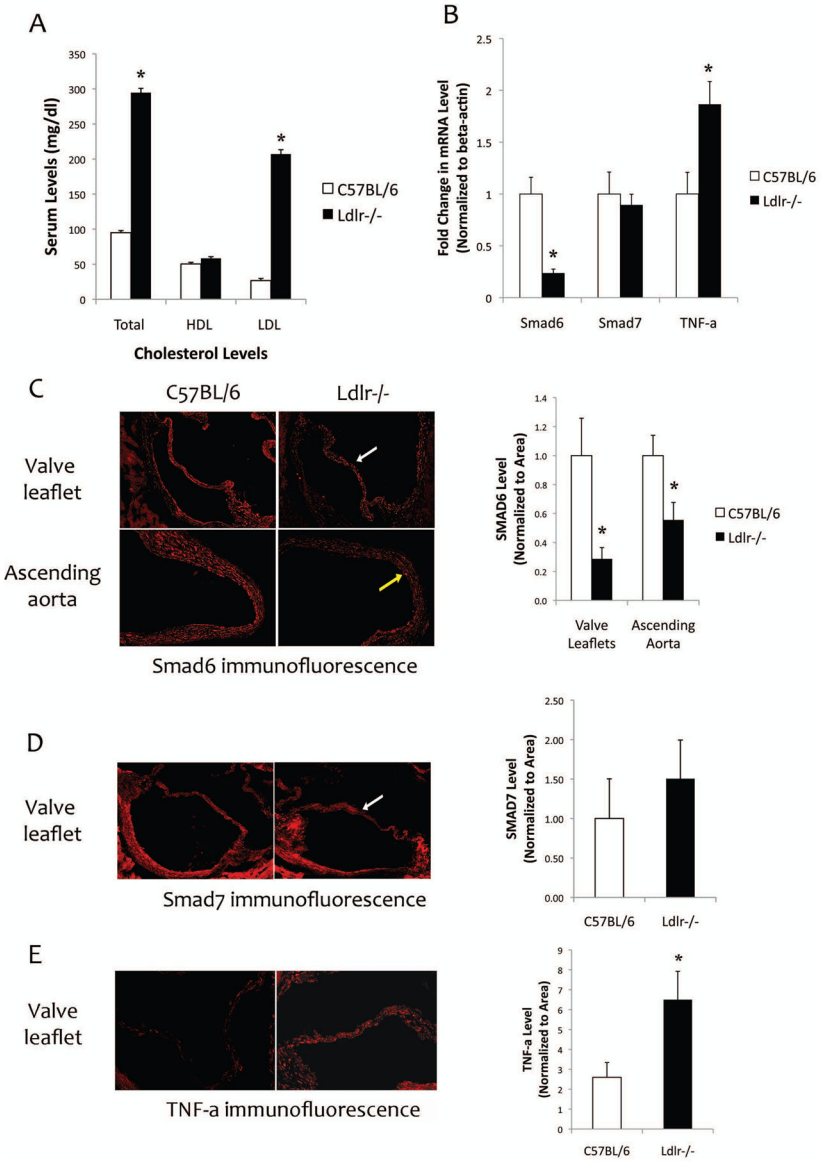

Figure 1. Expression of I-Smads and TNF-a in aortic tissues of normolipemic and hyperlipidemic mice

(A) Serum cholesterol levels of C57BL/6 and *Ldlr*$^{-/-}$ mice. (B) Realtime RT-qPCR analysis of aortic tissues from C57BL/6 and *Ldlr*$^{-/-}$ mice for Smad6, Smad7, and TNF-a expression. $^{*}p < 0.05$ *vs.* respective C57BL/6 controls. (C) Left - Immunofluorescence images of aortic valve leaflets (white arrow) and aorta (yellow arrow) from C57BL/6 (n = 7) and *Ldlr*$^{-/-}$ (n= 7) mice for Smad6. Magnification: 10X. Right - Quantitation of the images (normalized per tissue area) using image analysis software (Metamorph Advanced *v*7.7). $^{*}p < 0.05$ *vs.* respective C57BL/6 controls. (D) Left - Immunofluorescence images of aortic valve leaflets (white arrow) from C57BL/6 (n = 6) and *Ldlr*$^{-/-}$ (n= 6) mice for Smad7. Right - Quantitation of the images (normalized per tissue area) using the image analysis software. (E) Left - Immunofluorescence images of aortic valve leaflets from C57BL/6 (n = 7) and

Ldlr$^{-/-}$ (n= 7) mice for TNF-a. Right - Quantitation of the images (normalized per tissue area) using the image analysis software. $^{*}p < 0.05$ *vs.* respective C57BL/6 controls.

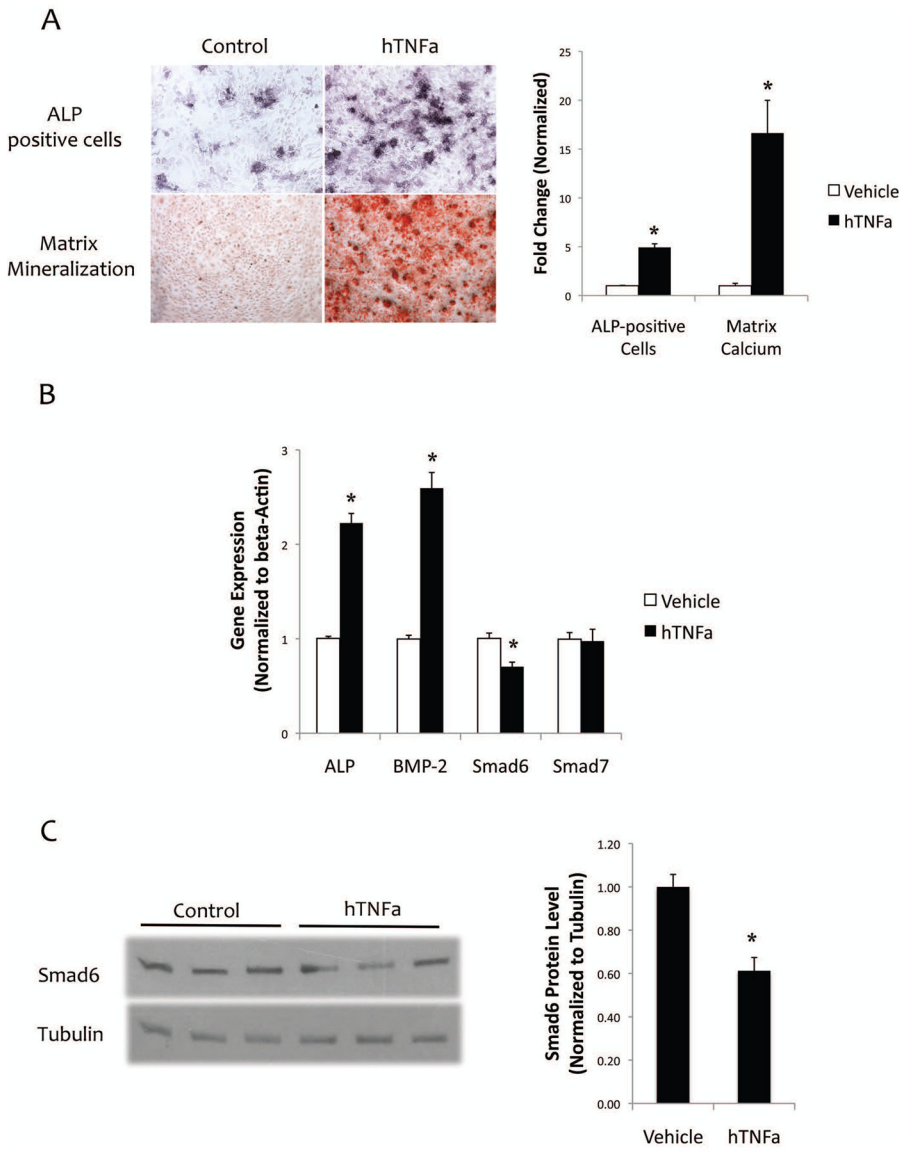

Figure 2. Effects of TNF-a on osteoblastic differentiation and mineralization

(A) Left - Cytochemical staining for ALP activity (purple) and alizarin red staining for matrix calcium (red) in response to hTNF-a (25 ng/ml) for 6 and 18 days of treatment, respectively. Magnification – 10X. Right - Quantitative analysis of ALP-positive cells (normalized to cell number) and *o*-cresolphthalein complexone for matrix calcium (normalized to protein) in response to hTNF-a (25 ng/ml) treatment. $^{*}p < 0.05$ *vs.* respective control vehicle. (B) Realtime RT-qPCR analysis of ALP, BMP-2, Smad6, and Smad7 expression in response to hTNF-a (25 ng/ml) treatment for 10 days. $^{*}p < 0.05$ *vs.* respective control vehicle (C) Left -Western blot analysis of Smad6 in response to hTNF-a (25 ng/ml) treatment for 10 days. Right - Quantitative analysis of the Western blot using NIH Image J *v64*. $^{*}p < 0.05$ *vs.* control vehicle.

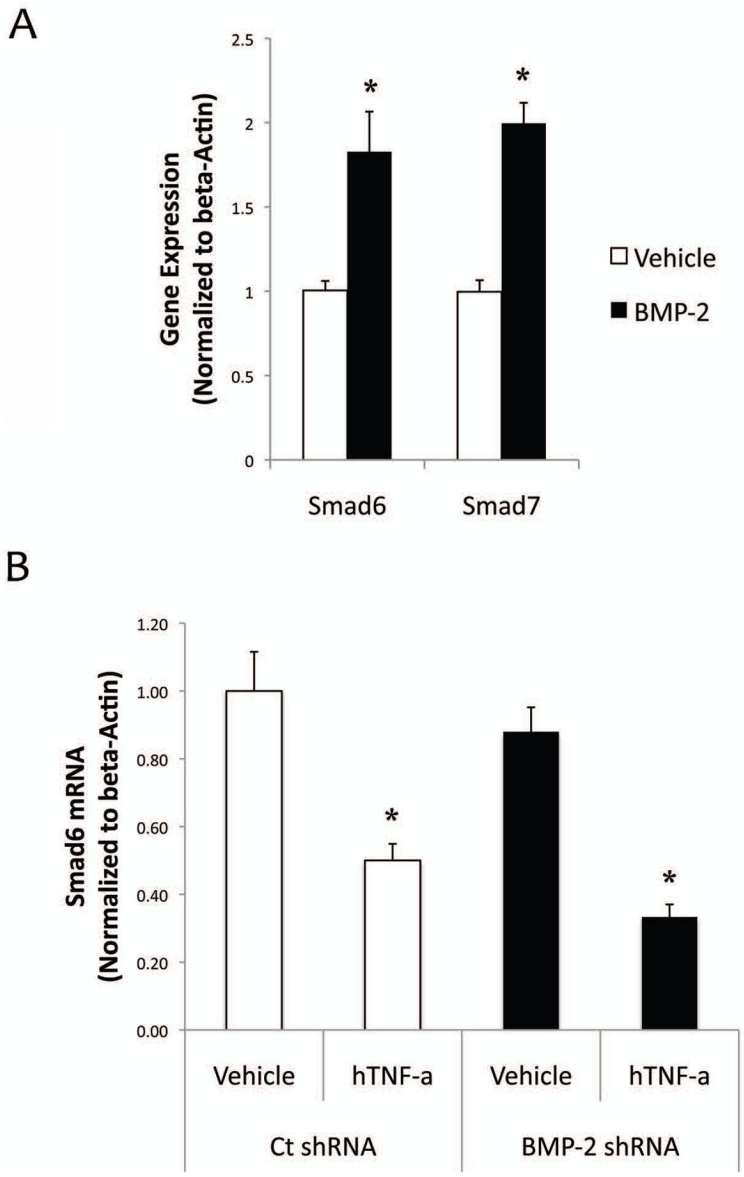

Figure 3. Effects of BMP-2 on Smad expression

(A) Realtime RT-qPCR analysis of Smad6 and Smad7 expression in response to BMP-2 (100 ng/ml) treatment for 10 days. $^{*}p < 0.05$ *vs.* respective control vehicle. (B) Realtime RT-qPCR analysis of Smad6 expression in control shRNA or BMP-2 shRNA. $^{*}p < 0.05$ *vs.* respective control vehicle.

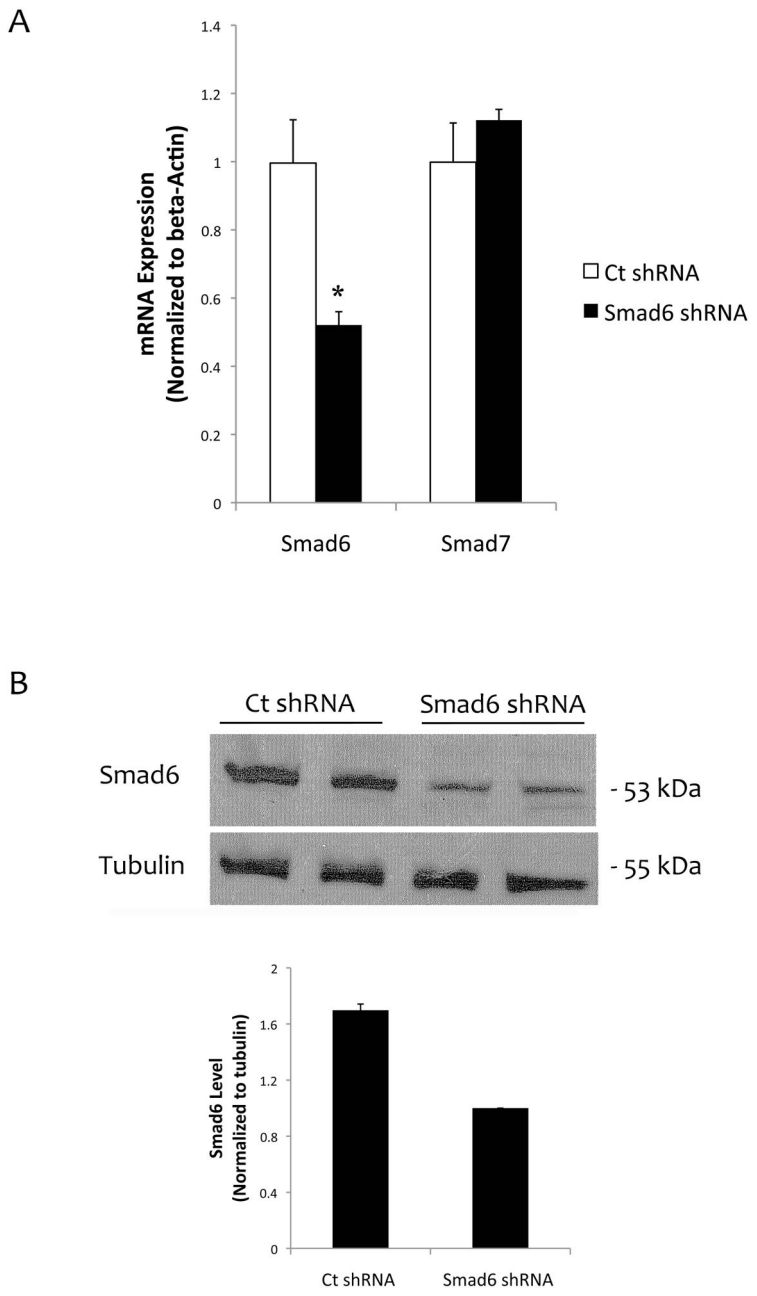

Figure 4. Knocking down Smad6 in mVICs

(A) Realtime RT-qPCR analysis for Smad6 and Smad7 expression in mVICs transfected with control shRNA or Smad6 shRNA. $^{*}p < 0.05$ vs. respective control. (B) Western analysis of cell lysates from mVICs transfected with control shRNA or Smad6 shRNA. Tubulin was used as a loading control. Quantitative analysis of the lanes via NIH Image J *v64* is shown in a graph.

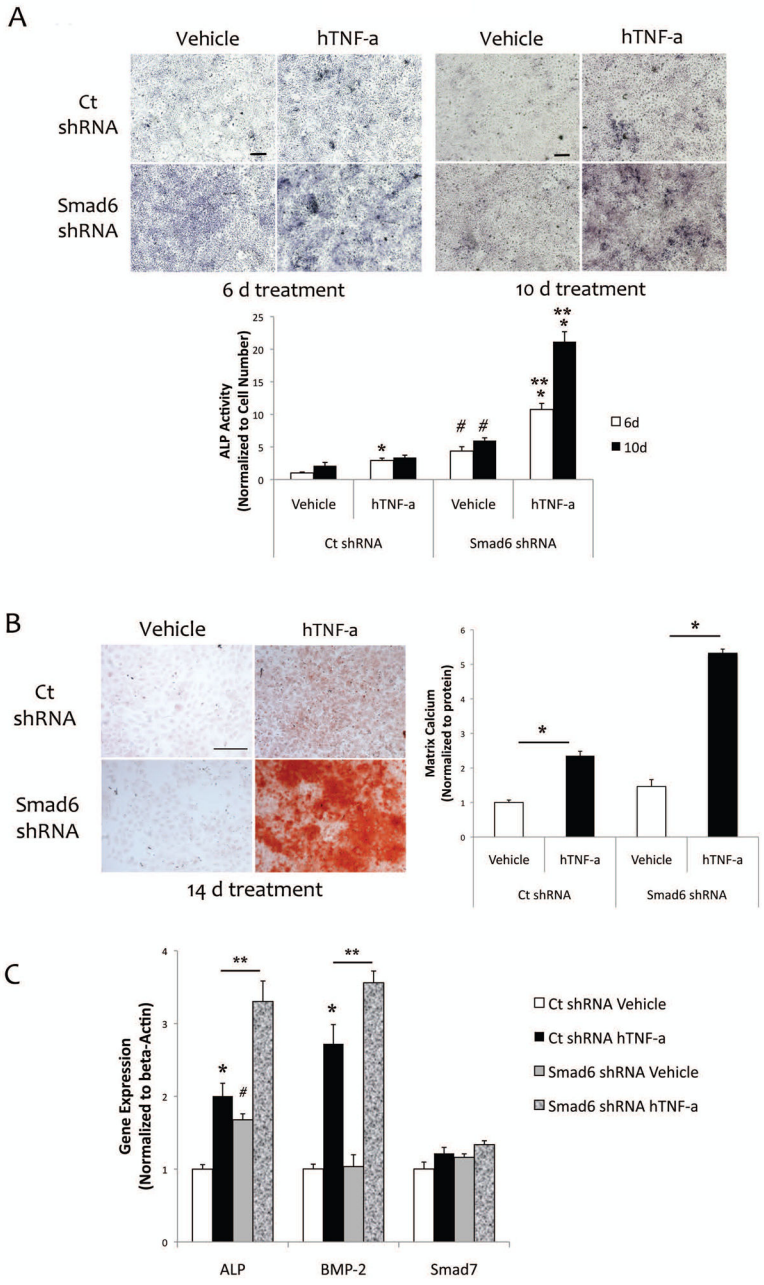

Figure 5. Effects of Smad6 knockdown on TNF-a-induced osteoblastic differentiation and mineralization in mVIC

(A) Cytochemical staining for ALP activity (purple) in response to hTNF-a (25 ng/ml). Scale bar – 200μ. Quantitative analysis is shown in the lower panel. $^{*}p < 0.05$ vs. respective vehicle control at each time point; $^{\#}p < 0.05$ vs. respective ct shRNA at each time point; $^{**}p < 0.05$ vs. ct shRNA hTNF-a. (B) Left - Alizarin red staining for matrix calcium in response to hTNF-a (25 ng/ml). Magnification – 4X. Right - *O*-cresolphthalein complexone analysis for matrix calcium (normalized to protein) in response to hTNF-a for 14 days. $^{*}p < 0.05$ vs. respective vehicle control. (C) Realtime RT-qPCR analysis of ALP, BMP-2, and Smad7

expression in response to hTNF-a (25 ng/ml) for 6 days. $^{*}p < 0.05$ vs. respective vehicle control; $^{\#}p < 0.05$ vs. ct shRNA vehicle; $^{**}p < 0.05$ vs. ct shRNA hTNF-a.

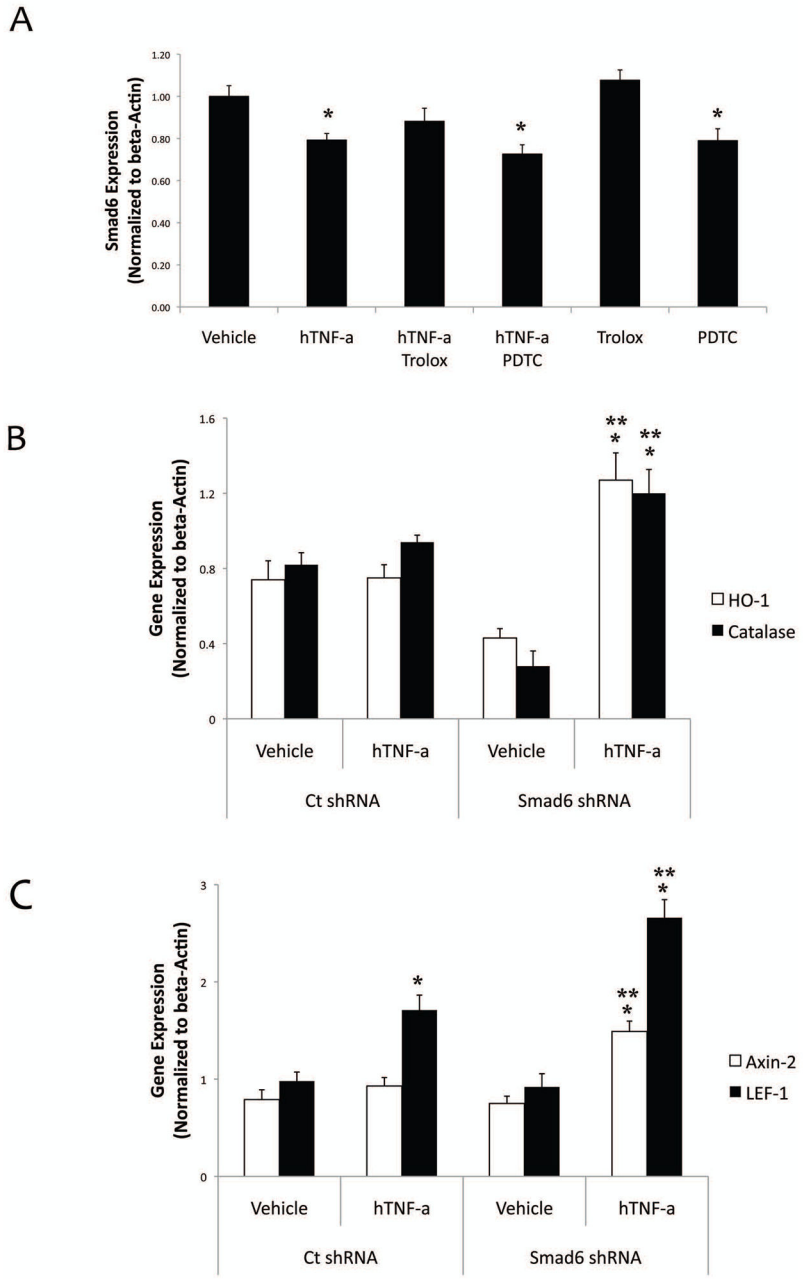

Figure 6. Effects of Smad6 knockdown on TNF-a-induced oxidative stress and Wnt signaling in mVIC

(A) Realtime RT-qPCR analysis of Smad6 expression in response to hTNF-a (25 ng/ml), Trolox (400 μM) or PDTC (10 μM), as indicated, for 10 days. Cells were cotreated with PDTC or pretreated with trolox for 1 hr prior to TNF-a addition at each media change. $^{*}p < 0.05$ vs. vehicle control (B) Realtime RT-qPCR analysis of hemeoxygenase-1 (HO-1) and catalase expression in response to hTNF-a (25 ng/ml) for 10 days. $^{*}p < 0.05$ vs. respective vehicle control; $^{**}p < 0.05$ vs. ct shRNA hTNF-a. (C) Realtime RT-qPCR analysis of Wnt

downstream targets Axin-2 and LEF-1 expression in response to hTNF-a (25 ng/ml) for 10 days. $^{*}p < 0.05$ vs. respective vehicle control; $^{**}p < 0.05$ vs. ct shRNA hTNF-a.